Anal. Chem. **2008,** *80,* 3522–3529

High-Throughput Single Copy DNA Amplification and Cell Analysis in Engineered Nanoliter Droplets

Palani Kumaresan,[†] Chaoyong James Yang,[‡,||] Samantha A. Cronier,[§] Robert G. Blazej,[§] and Richard A. Mathies*[,‡,§]

Department of Mechanical Engineering, Department of Chemistry, and UCSF/UC Berkeley Joint Bioengineering Graduate Group, University of California, Berkeley, California 94720

A high-throughput single copy genetic amplification (SCGA) process is developed that utilizes a microfabricated droplet generator (*μ*DG) to rapidly encapsulate individual DNA molecules or cells together with primer functionalized microbeads in uniform PCR mix droplets. The nanoliter volume droplets uniquely enable quantitative high-yield amplification of DNA targets suitable for long-range sequencing and genetic analysis. A hybrid glass−polydimethylsiloxane (PDMS) microdevice assembly is used to integrate a micropump into the *μ*DG that provides uniform droplet size, controlled generation frequency, and effective bead incorporation. After bulk PCR amplification, the droplets are lysed and the beads are recovered and rapidly analyzed via flow cytometry. DNA targets ranging in size from 380 to 1139 bp at single molecule concentrations are quantitatively amplified using SCGA. Long-range sequencing results from beads each carrying ∼100 amol of a 624 bp product demonstrate that these amplicons are competent for achieving attomole-scale Sanger sequencing from a single bead and for advancing pyrosequencing read-lengths. Successful single cell analysis of the glyceraldehyde 3 phosphate dehydrogenase (GAPDH) gene in human lymphocyte cells and of the *gyr B* gene in bacterial *Escherichia coli* K12 cells establishes that SCGA will also be valuable for performing high-throughput genetic analysis on single cells.

DNA sequencing with both high accuracy and long-range contiguity will continue to play a central role in furthering our understanding of speciation, evolution, disease, and cancer for years to come.[1–3] Recent work by Levy et al.,[4] detailing a comparison between the two sets of chromosomes from one individual's diploid genome, shows that human genetic variation is as much as 5 times larger than the 0.1% previously estimated[5] and that structural variations such as block substitutions, insertions, inversions, deletions, and duplications constitute the majority (74%) of the variant bases rather than single nucleotide polymorphisms (SNPs). Structural variations (SVs) have been linked to a variety of genomic disorders such as Williams−Beuren syndrome, velocardiofacial syndrome,[6,7] and phenotypic variations such as those leading to systemic autoimmunity[8] and susceptibility to HIV infection.[9] Although de novo sequencing of more than 1400 complex genomes continues at an astounding rate, only 23 eukaryotic genome assemblies are completed to date due in large part to the cost and throughput constraints of current DNA sequencing techniques [NCBI Entrez Genome Project (2007) www.ncbi.nlm.nih.gov]. To enhance complex genome sequencing capability, it is important to develop next-generation low-cost technologies[10–12] that advance both short-range and long-range sequencing.

All next-generation sequencing techniques begin by eliminating the cloning-based DNA library preparation. One-step in vitro amplification of sheared genomic fragments on microbeads using microemulsion technology has emerged as a rapid, low-cost

* Corresponding author. Department of Chemistry, MS 1460, University of California, Berkeley, CA, 94720. Phone: (510) 642-4192. Fax: (510) 642-3599. E-mail: rich@zinc.cchem.berkeley.edu.

[†] Department of Mechanical Engineering.

[‡] Department of Chemistry.

[§] UCSF/UC Berkeley Joint Bioengineering Graduate Group.

[||] Current address: College of Chemical Engineering, Xiamen University, Xiamen 631005, P. R. China.

(1) Loftus, B. J.; Fung, E.; Roncaglia, P.; Rowley, D.; Amedeo, P.; Bruno, D.; Vamathevan, J.; Miranda, M.; Anderson, I. J.; Fraser, J. A.; Allen, J. E.; Bosdet, I. E.; Brent, M. R.; Chiu, R.; Doering, T. L.; Dontin, M. J.; D'Souza, C. A.; Fox, D. S.; Grinberg, V.; Fu, J. M.; Fukushima, M.; Haas, B. J.; Huang, J. C.; Janbon, G.; Jones, S. J. M.; Koo, H. L.; Krzywinski, M. I.; Kwon-Chung, J. K.; Lengeler, K. B.; Maiti, R.; Marra, M. A.; Marra, R. E.; Mathewson, C. A.; Mitchell, T. G.; Pertea, M.; Riggs, F. R.; Salzberg, S. L.; Schein, J. E.; Shvartsbeyn, A.; Shin, H.; Shumway, M.; Specht, C. A.; Suh, B. B.; Tenney, A.; Utterback, T. R.; Wickes, B. L.; Wortman, J. R.; Wye, N. H.; Kronstad, J. W.; Lodge, J. K.; Heitman, J.; Davis, R. W.; Fraser, C. M.; Hyman, R. W. *Science* **2005**, *307*, 1321–1324.

(2) Check, E. *Nature* **2005**, *437*, 1084–1086.

(3) Zhao, S. Y.; Shetty, J.; Hou, L. H.; Delcher, A.; Zhu, B. L.; Osoegawa, K.; de Jong, P.; Nierman, W. C.; Strausberg, R. L.; Fraser, C. M *Genome Res.* **2004**, *14*, 1851–1860.

(4) Levy, S.; Sutton, G.; Ng, P. C.; Feuk, L.; Halpern, A. L.; Walenz, B. P.; Axelrod, N.; Huang, J.; Kirkness, E. F.; Denisov, G.; Lin, Y.; Macdonald, J. R.; Pang, A. W.; Shago, M.; Stockwell, T. B.; Tsiamouri, A.; Bafna, V.; Bansal, V.; Kravitz, S. A.; Busam, D. A.; Beeson, K. Y.; McIntosh, T. C.; Remington, K. A.; Abril, J. F.; Gill, J.; Borman, J.; Rogers, Y. H.; Frazier, M. E.; Scherer, S. W.; Strausberg, R. L.; Venter, J. C. *PLoS Biol.* **2007**, *5*, e254.

(5) The International HapMap, C *Nature* **2005**, *437*, 1299–1320.

(6) Lupski, J. R.; Stankiewicz, P. *PLoS Genetics* **2005**, *1*, e49.

(7) Freeman, J. L.; Perry, G. H.; Feuk, L.; Redon, R.; McCarroll, S. A.; Altshuler, D. M.; Aburatani, H.; Jones, K. W.; Tyler-Smith, C.; Hurles, M. E.; Carter, N. P.; Scherer, S. W.; Lee, C. *Genome Res.* **2006**, *16*, 949–961.

(8) Fanciulli, M.; Norsworthy, P. J.; Petretto, E.; Dong, R.; Harper, L.; Kamesh, L.; Heward, J. M.; Gough, S. C. L.; de Smith, A.; Blakemore, A. I. F.; Owen, C. J.; Pearce, S. H. S.; Teixeira, L.; Guillevin, L.; Graham, D. S. C.; Pusey, C. D.; Cook, H. T.; Vyse, T. J.; Aitman, T. J. *Nat. Genet.* **2007**, *39*, 721–723.

(9) Gonzalez, E.; Kulkarni, H.; Bolivar, H.; Mangano, A.; Sanchez, R.; Catano, G.; Nibbs, R. J.; Freedman, B. I.; Quinones, M. P.; Bamshad, M. J.; Murthy, K. K.; Rovin, B. H.; Bradley, W.; Clark, R. A.; Anderson, S. A.; O'Connell, R. J.; Agan, B. K.; Ahuja, S. S.; Bologna, R.; Sen, L.; Dolan, M. J.; Ahuja, S. K. *Science* **2005**, *307*, 1434–1440.

10.1021/ac800327d CCC: $40.75
Published on Web 04/15/2008

alternative.[10] However, this approach suffers from nonuniform amplification and is limited to short DNA amplicons (~250 bp) due to the small and variable volume (1~100 pL) of the emulsions. The ability to uniformly generate attomole quantities of long DNA amplicons (>600 bp) from a single molecule in a high-throughput manner would significantly enhance DNA sequencing. For example, such amplicons could serve as the template for Sanger DNA sequencing, which can now be performed using only 100 amol of PCR product,[13] and they could provide the uniform long templates needed to enhance read lengths of cyclic array sequencing methods.[10,14]

The transition from emulsions produced by conventional mechanical agitation to the generation of monodisperse aqueous-in-oil droplets using microfluidic systems[15] has the potential to dramatically advance the utility of a wide variety of emulsion-based chemistries. Microfluidics enables not only high-throughput droplet production but also precise control over the droplet size and hence, reaction volume. Such droplets have been used in a variety of biological and chemical applications including DNA analyses,[16] viral RNA analyses,[17] protein crystallization,[18] organic synthesis, [19] and nanoparticle synthesis.[20] Droplets generated by microfluidic systems are ideal for amplifying a genomic library because the droplet volume is under precise control and is sufficiently large to efficiently and uniformly amplify long fragments of interest.

The production of uniform droplet reactors for genetic amplification is also valuable for the analyses of cellular genetics. Individual cells encapsulated in picoliter to nanoliter volume droplets in a high-throughput manner will enable digital studies of genetic and gene expression variations at the single cell level over a large population of cells. For example, mutations and transcript variations that lead to various cancers could be understood at the single cell level without the population averaging of homogenized samples. Thus far, only low-throughput encapsulation of cells in droplets has been successfully shown.[21,22]

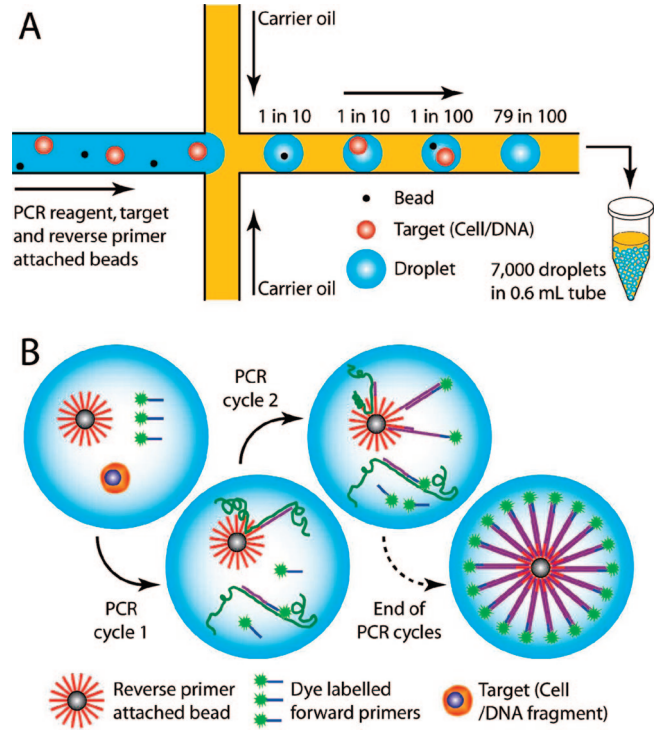

Figure 1. Single copy genetic amplification (SCGA): (A) target DNA or cells and beads are mixed with the PCR reagent (blue) at very dilute concentrations and pumped through a microfabricated droplet generator (μDG). Monodisperse nanoliter volume droplets of the PCR reagent are formed in a carrier oil (yellow) at the cross-injector and routed into a tube for temperature cycling. The number of droplets containing a single bead and a single target DNA/cell is controlled by varying their concentrations in the PCR solution and by controlling the droplet volume. (B) Each functional PCR mix droplet contains a bead covalently labeled with the reverse primer, dye labeled forward primer, and a single target copy. Subsequent steps of PCR generate dye labeled double stranded product on the bead surface. Following emulsion PCR, the droplets are broken and the beads are analyzed by flow cytometry to quantify the bound clonal amplified product.

Figure 1 presents a schematic of our single copy genetic amplification (SCGA) process that provides efficient high-throughput DNA amplification from a single template copy in individual droplets. Central to SCGA is the microfabricated droplet generator (μDG) that rapidly forms uniform volume reaction droplets in an immiscible carrier oil at the cross-injector (Figure 1A). The tunable 2−5 nL droplets comprise an aqueous reaction mixture, such as PCR reagent. A single target DNA molecule or cell is encapsulated in individual reaction droplets by introducing it at very dilute concentrations in the PCR reagent. Thousands of such droplets, generated at the cross-injector within minutes, are collected in a standard reaction tube and temperature cycled in parallel for high-throughput. In order to effectively isolate and analyze products amplified from distinct DNA templates in individual droplets, reverse primer functionalized microbeads are incorporated in the droplets along with the target. Figure 1B schematically shows the first two cycles and the final result of

(10) Margulies, M.; Egholm, M.; Altman, W. E.; Attiya, S.; Bader, J. S.; Bemben, L. A.; Berka, J.; Braverman, M. S.; Chen, Y. J.; Chen, Z. T.; Dewell, S. B.; Du, L.; Fierro, J. M.; Gomes, X. V.; Godwin, B. C.; He, W.; Helgesen, S.; Ho, C. H.; Irzyk, G. P.; Jando, S. C.; Alenquer, M. L. I.; Jarvie, T. P.; Jirage, K. B.; Kim, J. B.; Knight, J. R.; Lanza, J. R.; Leamon, J. H.; Lefkowitz, S. M.; Lei, M.; Li, J.; Lohman, K. L.; Lu, H.; Makhijani, V. B.; McDade, K. E.; McKenna, M. P.; Myers, E. W.; Nickerson, E.; Nobile, J. R.; Plant, R.; Puc, B. P.; Ronan, M. T.; Roth, G. T.; Sarkis, G. J.; Simons, J. F.; Simpson, J. W.; Srinivasan, M.; Tartaro, K. R.; Tomasz, A.; Vogt, K. A.; Volkmer, G. A.; Wang, S. H.; Wang, Y.; Weiner, M. P.; Yu, P. G.; Begley, R. F.; Rothberg, J. M. *Nature* **2005**, *437*, 376–380.

(11) Shendure, J.; Porreca, G. J.; Reppas, N. B.; Lin, X. X.; McCutcheon, J. P.; Rosenbaum, A. M.; Wang, M. D.; Zhang, K.; Mitra, R. D.; Church, G. M. *Science* **2005**, *309*, 1728–1732.

(12) Blazej, R. G.; Kumaresan, P.; Mathies, R. A. *Proc. Natl. Acad. Sci. U.S.A.* **2006**, *103*, 7240–7245.

(13) Blazej, R. G.; Kumaresan, P.; Cronier, S. A.; Mathies, R. A. *Anal. Chem.* **2007**, *79*, 4499–4506.

(14) Seo, T. S.; Bai, X. P.; Kim, D. H.; Meng, Q. L.; Shi, S. D.; Ruparelt, H.; Li, Z. M.; Turro, N. J.; Ju, J. Y. *Proc. Natl. Acad. Sci. U.S.A.* **2005**, *102*, 5926–5931.

(15) Song, H.; Chen, D. L.; Ismagilov, R. F. *Angew. Chem., Int. Ed.* **2006**, *45*, 7336–7356.

(16) Beer, N. R.; Hindson, B. J.; Wheeler, E. K.; Hall, S. B.; Rose, K. A.; Kennedy, I. M.; Colston, B. W. *Anal. Chem.* **2007**, *79*, 8471–8475.

(17) Beer, N. R.; Wheeler, E. K.; Lee-Houghton, L.; Watkins, N.; Nasarabadi, S.; Hebert, N.; Leung, P.; Arnold, D. W.; Bailey, C. G.; Colston, B. W. *Anal. Chem.* **2008**, *80*, 1854–1858.

(18) Zheng, B.; Gerdts, C. J.; Ismagilov, R. F. *Curr. Opin. Struct. Biol.* **2005**, *15*, 548–555.

(19) Burns, J. R.; Ramshaw, C. *Lab Chip* **2001**, *1*, 10–15.

(20) Chan, E. M.; Alivisatos, A. P.; Mathies, R. A. *J. Am. Chem. Soc.* **2005**, *127*, 13854–13861.

(21) He, M. Y.; Edgar, J. S.; Jeffries, G. D. M.; Lorenz, R. M.; Shelby, J. P.; Chiu, D. T. *Anal. Chem.* **2005**, *77*, 1539–1544.

(22) Tan, Y. C.; Hettiarachchi, K.; Siu, M.; Pan, Y. R.; Lee, A. P. *J. Am. Chem. Soc.* **2006**, *128*, 5656–5658.

PCR in a droplet containing one bead and one target. Dye-labeled double-stranded amplicons are produced on the bead surface, which allow downstream quantitation of the amount of PCR product. Using the system developed here, we show that it is possible to produce ~100 amol of >600 bp DNA amplicon on individual beads from a single template copy. This improved yield of long DNA products is ideally suited for miniaturized Sanger sequencing as well as long-read pyrosequencing. We also perform single mammalian and bacterial cell genetic analysis at stochastic level dilutions of the cells, establishing the capability to perform high-throughput single cell genetic analysis.

EXPERIMENTAL SECTION

***μ*DG Fabrication and Preparation.** The four layer *μ*DG is constructed from three glass wafers and a featureless PDMS membrane following a process similar to that described by Grover et al.[23] After fabrication, the cross-injector (Figure 2A) is rendered hydrophobic with octadecyltrichlorosilane (OTS) treatment, and fluidic connections between carrier oil[10] filled syringes and the device are made using microtubings, custom ferrules, and custom aluminum manifolds.

Bead and PCR Mix Preparation. Microbeads are prepared by linking reverse primers to 34 *μ*m mean diameter agarose beads via amine−NHS conjugation chemistry.[10] The bead concentration is determined using a hemacytometer, and the amount of reverse primer covalently linked to a bead is quantified by annealing FAM-labeled cDNA to the reverse primers and measuring the fluorescence intensity using flow cytometry. A volume of 100 *μ*L of the PCR mix containing ~6600 reverse primer functionalized beads and varying amounts of template DNA or cell is prepared in a 0.6 mL PCR tube for each of the reaction conditions. Emulsion droplets (50 *μ*L) are collected in three separate tubes holding correspondingly equal volumes of microfine solution.[10]

Droplet PCR and Product Quantitation. The pumping region of the *μ*DG is treated with a coating solution prior to droplet generation to minimize DNA/polymerase adsorption on the glass and PDMS surface. Following this, droplets are generated by infusing the carrier oil using a syringe pump and the PCR mix using the on-chip PDMS membrane pump. The on-chip pump operating at 5.7 Hz generates one 2.5 nL droplet every pumping cycle. Approximately 6600 droplets are collected in each of the three 0.6 mL PCR tubes containing microfines and simultaneously temperature cycled 40 times. Beads are recovered from the droplets after thermal cycling following a technique previously reported by Margulies et al.[10] They are then analyzed using a flow cytometer with a 488 nm excitation source. Beads with different known amounts of fluorophores are used as a standard to quantify FAM-labeled DNA product on processed beads. (see Supporting Information for detailed methods)

RESULTS

***μ*DG Operation.** The *μ*DG shown in Figure 2A is a four-layer sandwich consisting of a blank glass wafer, a microfabricated glass fluidic wafer, a featureless PDMS membrane, and a microfabricated manifold wafer. The enclosed all-glass channels (black) are formed by thermally bonding the blank wafer to the patterned

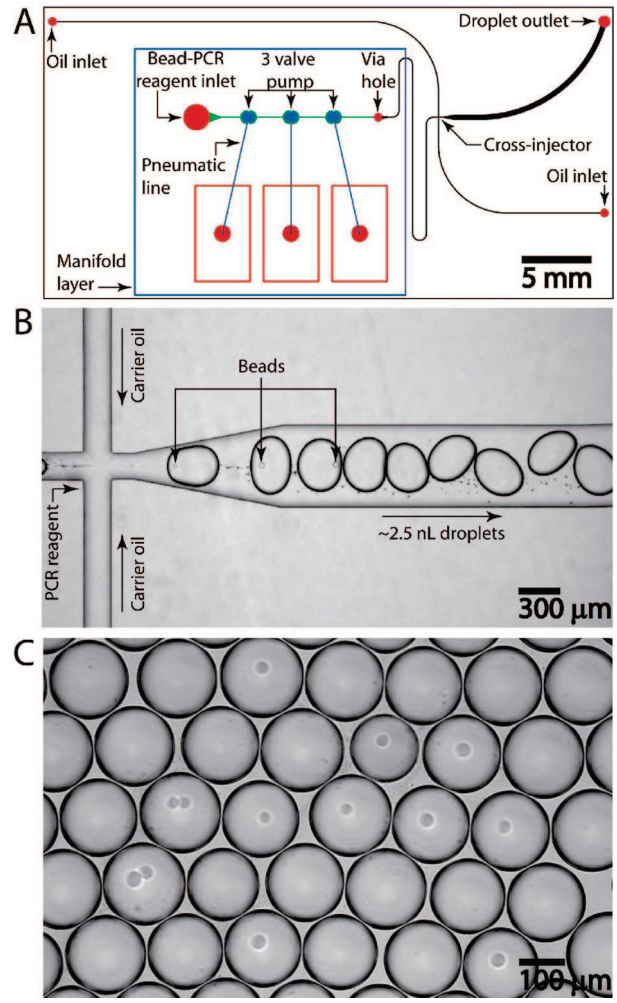

Figure 2. *μ*DG for controlled formation of nanoliter PCR droplets. (A) Layout of the device, showing the PCR solution inlet, the two oil inlets, and the droplet outlet ports (red). A three layer (glass−PDMS−glass) pneumatically controlled micropump is integrated on-chip to deliver PCR reagent containing dilute 34 *μ*m beads and template. The manifold layer (blue) controls valve actuation, and the via hole connects the glass−PDMS hybrid channel (green) to the thermally bonded all-glass channel and cross-injector (black). Etch depth, 100 *μ*m. (B) Optical micrograph of droplet generation at the cross-injector. Droplets are generated at a frequency of 5.7 Hz with a combined oil flow rate of 2.2 *μ*L/min and a PCR solution flow rate of 0.8 *μ*L/min. For this experiment, average bead concentration was 130 beads/*μ*L (0.33 bead/droplet). (C) Optical micrograph of droplets with a predictable stochastic distribution of beads.

side of the fluidic wafer. The diced bottom stack is contact bonded by the PDMS membrane to the manifold wafer (blue), forming the microvalves and a three-dimensional fluidic interconnect. Pressure and vacuum signals are transferred by the pneumatic control lines (blue) to the three microvalves, which pump PCR reagent containing target and beads through the "via" hole (red) into the all-glass channel. A syringe pump is used to continuously infuse carrier oil into the all-glass channels through the two oil inlet ports. An optical micrograph of droplet formation at the cross-injector is presented in Figure 2B. The droplet generation corresponds precisely with the on-chip pumping frequency because it is determined by the pulsatile nature of the on-chip pump. The process of droplet separation also results in the formation of minute droplets or microfines (~femtoliters) that can

(23) Grover, W. H.; Skelley, A. M.; Liu, C. N.; Lagally, E. T.; Mathies, R. A. *Sens. Actuators, B* **2003**, *89*, 315–323.

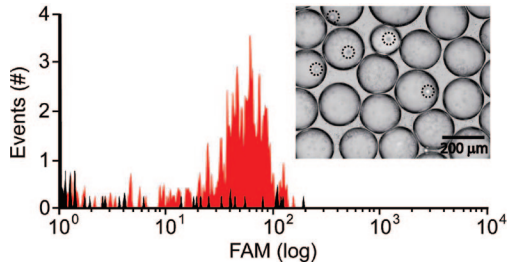

Figure 3. Emulsion droplet thermostability test. The red plot (events versus log of FAM intensity) presents flow cytometry analysis of the positive control, comprising beads from temperature-cycled emulsion droplets formed with all necessary PCR components. The black plot corresponds to beads produced from a mixture of two populations of emulsion droplets: one contained all PCR components minus the forward primer and another with all PCR components minus the reverse primer and reverse primer labeled beads. (Inset) Image of emulsion droplets containing beads after 40 cycles of PCR. Microbeads in the droplets are highlighted with dashed circles. The PCR target is a 380 bp amplicon from the pUC18 plasmid, and the template concentration is 10 molecules/2.5 nL droplet.

be seen as dark specks in Figure 2B. The maximum frequency at which beads are consistently incorporated into the droplets without being trapped in the microvalves is ~6 Hz. Figure 2C presents an array of droplets formed with a stochastic distribution of beads (26% of droplets with ≥ 1 bead) collected from the μDG and displayed on a glass slide. The droplets show a highly uniform diameter of 167 ± 6 μm that corresponds to a volume of 2.4 nL with a variance of only 0.3 nL.

Thermostability of Emulsion Droplets. SCGA requires stable emulsion droplets and the absence of any DNA exchange during temperature cycling. Droplet stability was tested by forming two sets of emulsion droplets, each lacking one essential PCR component that is present in the other, followed by pooled thermocycling. The pUC18 plasmid at a concentration of 10 molecules per 2.5 nL droplet is used as the template. A first set of PCR solution droplets is formed without the dye labeled pUC18 380 bp forward primer (Table S-1); the second set is formed without the reverse primer conjugated beads. Figure 3 presents flow cytometry results for the beads (black plot) after temperature cycling 40 times. Only 2% of the beads show fluorescence equivalent to the beads from the control (red plot), where all components are included in the PCR solution. This is likely due to droplet merger that occurs when the droplet outlet tubing from the μDG is reinserted into the PCR tube to collect the second set of droplets. Emulsion droplet thermostability following 40 PCR cycles is also visually verified (Figure 3, inset). Droplets bigger than ~5 nL were found to merge upon thermal cycling.

Single Molecule Genetic Amplification. To explore copy number effects on amplification efficiency, a 380 bp region of the pUC18 plasmid was amplified at four different template dilutions (0, 0.1, 1, and 10 copies per 2.5 nL droplet). Figure 4A presents the flow cytometry results for the respective conditions. At 0 template/droplet concentration, a majority of beads have low fluorescence intensity. Less than 3% of the beads display fluorescence values between 1 and 10 on the logarithmic FAM scale. Beads thermocycled in PCR solution droplets without the polymerase show similar results (data not shown), suggesting the low intensity is due to residual adsorption of FAM labeled primers on the beads and does not result from nonspecific amplification. At 0.1 template/droplet concentration, a brighter product peak (>10 FAM) is observed. The bright beads carry ~5 amol of DNA amplicon and make up ~5% of the total population. For the single molecule template concentration of 1 template/droplet, 26% of the bead population lights up and the fluorescence intensity indicates that ~5.6 amol of DNA product is generated per bead. At 10 molecules/droplet, 80% of the beads fluoresce due to ~8.6 amol of amplified DNA product per bead. The bold plot connecting circular dots in Figure 4B illustrates that there is a weak dependence of bead droplet PCR yield (5−8 amol/bead) on template concentration. On the basis of the mean template copy number per "active" droplet (containing both bead and DNA template), average PCR efficiency values over 40 cycles of PCR are determined. The bold plot connecting square dots in Figure 4B shows that around 40% PCR efficiency is achieved for bead droplet PCR. Free solution bead PCR performed in the absence of emulsions or oil, but with equivalent template and bead concentrations (dash plots), produce consistently lower yields and efficiencies. This may be due to lower average effective template concentration in free solution and reduced accessibility of the beads to the PCR reagent as a result of bead settlement during cycling.

Sequencing Template Production by SCGA. The product size and yield from a single molecule makes our technique suitable for single molecule or single cell genetic analysis and sequencing.[11,21,24] Current techniques for high-throughput single molecule amplification based on conventional emulsion PCR methods produce ~10 amol of short amplicons (~250 bp) per bead.[10] However, for next generation de novo sequencing applications, such as the microbead integrated DNA sequencing (MINDS),[12] it is critical to amplify longer templates (500−1000 bp) at higher yields on a microbead. The amount of amplicon generated per bead needs to be in the 50−100 amol range to enable Sanger sequencing directly from individual beads.[13]

To address this need, microbeads with higher primer density were prepared. The ratio of amine functionalized reverse primers to beads in the conjugation reaction was increased from 4.3 to 20 fmol per bead, resulting in 4.4 fmol of primer being bound per bead. These beads were used to characterize the effect of amplicon size on bead droplet PCR yield. Approximately 175 amol of 380 bp DNA product is generated on each bead (Figure 5A) when starting with 10 pUC18 DNA molecules per droplet. A slight decrease in bead droplet PCR yield to ~155 amol is observed when the amplicon size is increased to 624 bp. For an 1139 bp amplicon, the PCR yield dropped to ~10 amol per bead. A possible explanation for this drop is greater molecular crowding with the longer DNA templates on the bead surface, resulting in reduced PCR efficiency.[25,26] The 624 bp size product, being a good target for Sanger sequencing, was also amplified in the single molecule limit (1 template/droplet) yielding 50−100 amol of amplicon per bead (Figure 5B) over four identical runs.

To determine whether these bead-amplified-templates are competent for Sanger extension, a dye-terminator sequencing reaction using ~600 beads from one of the runs was performed

(24) Dressman, D.; Yan, H.; Traverso, G.; Kinzler, K. W.; Vogelstein, B. *Proc. Natl. Acad. Sci. U.S.A.* **2003**, *100*, 8817–8822.
(25) Diehl, F.; Li, M.; He, Y. P.; Kinzler, K. W.; Vogelstein, B.; Dressman, D. *Nat. Methods* **2006**, *3*, 551–559.
(26) Mercier, J. F.; Slater, G. W. *Biophys. J.* **2005**, *89*, 32–42.

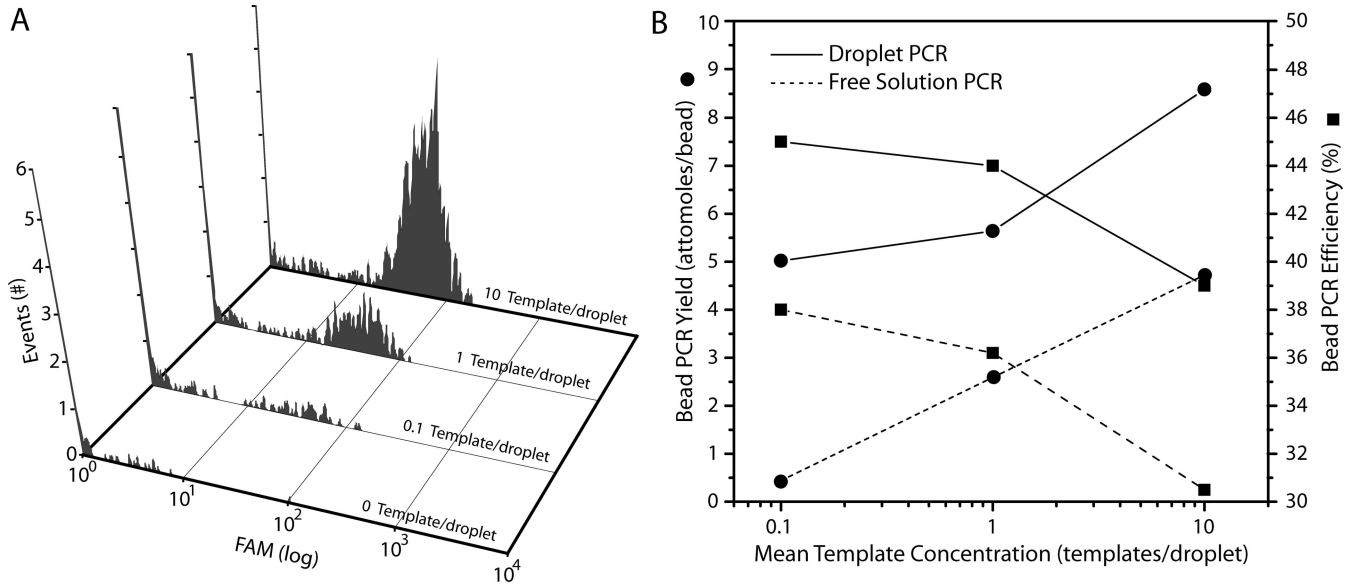

Figure 4. Microbead based emulsion droplet amplification of a 380 bp region from the pUC18 plasmid at four different template concentrations. (A) Flow cytometry analysis of microbeads from emulsion droplet PCR at an average template concentration of 10 molecules/droplet, 1 molecule/droplet, 0.1 molecule/droplet, and 0 molecule/droplet. (B) Bead PCR yield (●) and efficiency (■) in emulsion droplets (solid lines) for the different template concentrations. PCR yield and efficiency are calculated from active beads (beads corresponding with DNA template in a droplet). Free solution bead PCR results are shown using dashed lines. For each condition, ~20 000 droplets are formed, ~3 300 beads (75 amol of primer per bead) are processed, and ~700 beads are analyzed by flow cytometry.

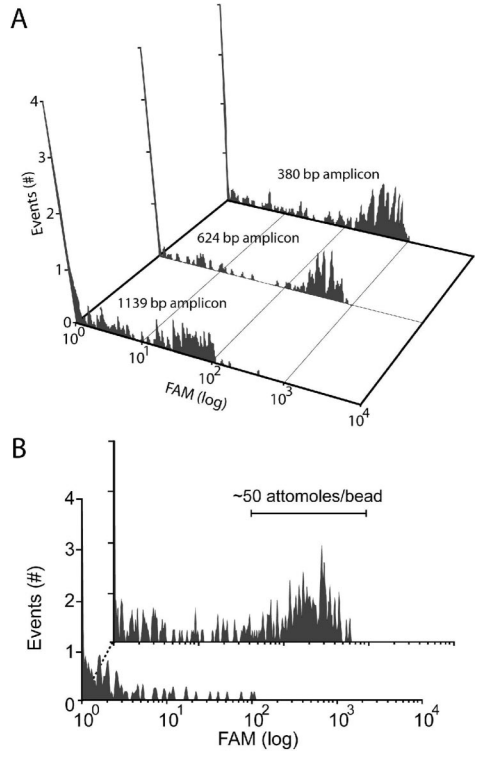

Figure 5. Amplification of DNA templates in emulsion droplets as a function of template length. (A) Comparison of PCR yields for 380 (~175 amol/bead), 624 (~155 amol/bead), and 1139 bp (~10 amol/bead) amplicons from a starting pUC18 template concentration of 10 molecules per droplet. (B) Flow cytometry analysis of beads carrying a 624 bp product amplified from 1 template per droplet (upper) and 0 template per droplet (lower). In this study, average reverse primer density per bead is 4.4 fmol.

on a standard thermal cycler. Unlabeled 24 bp forward PCR primer was used in the sequencing reaction, resulting in a maximum possible read length of 600 bases. The Sanger sequencing extension fragments were separated on a capillary array electrophoresis system (Figure S-1), and base call accuracies were predicted by PHRED.[27] Aggregate PHRED error rates estimate a read length of 554 bases at 99% accuracy (Figure S-2). Alternatively, a read length of 591 bases is produced using 99% accuracy cutoff with the known pUC18 sequence. Twenty one sequential "T" bases provided as spacers between the bead surface and amplicon to minimize steric hindrance are also successfully sequenced at the end of the 600 bases. The amine modified C_6 at the end of the poly-T bases (Table S-1) provides a ~1.5 nm separation between the last base sequenced and the bead surface. These data (summarized in Supporting Information results) demonstrating more than 500 bases of high quality sequence from DNA amplified on microbeads establish the capability of SCGA to generate sufficient amounts of long DNA on beads from a single template molecule to enable next generation Sanger [13,28] and pyrosequencing.

Single Cell Genetic Analysis. Successful SCGA from single cells requires that the high-frequency microvalve operation not compromise cell integrity. Mammalian cells (a lymphocyte cell line) were chosen as a critical test due to their fragile nature. Different known cell concentrations pumped through the μDG were collected, counted using flow cytometry, and compared with the number of cells in an equal volume of unprocessed solution. Figure 6A shows that at least 90% of the cells are recovered at various cell concentrations, indicating that on-chip pumping has little impact on cell integrity. The cells pumped through the μDG were also stained with Trypan blue and observed under a microscope, verifying their viability.

(27) Ewing, B.; Hillier, L.; Wendl, M. C.; Green, P. *Genome Res.* **1998**, *8*, 175–185.
(28) Fredlake, C. P.; Hert, D. G.; Kan, C. W.; Chiesl, T. N.; Root, B. E.; Forster, R. E.; Barron, A. E. *Proc. Natl. Acad. Sci. U.S.A.* **2008**, *105*, 476–481.

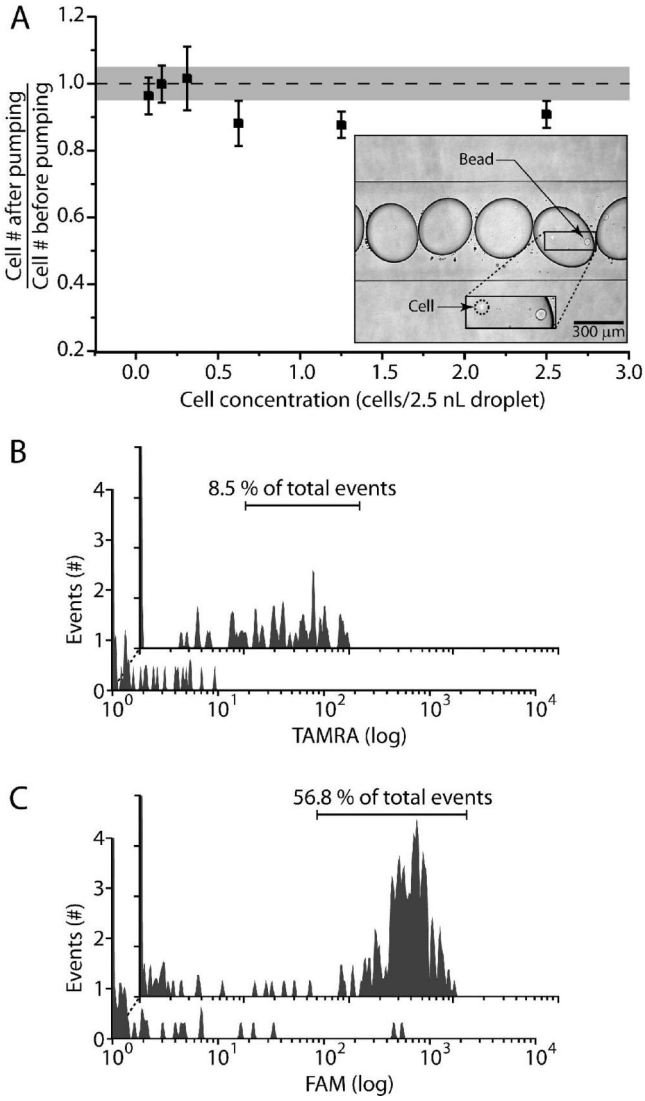

Figure 6. Single cell genetic analysis. (A) Comparison of the numbers of mammalian cells (human lymphocyte cell line) before and after pumping through the μDG at different cell concentrations. (A, inset) Optical micrograph of an emulsion droplet containing a single bead and a single mammalian cell. (B) Flow cytometry analysis of beads from emulsion droplet bead PCR, starting with 0.1 human lymphocyte cell/droplet (upper) and 0 human lymphocyte cell/droplet (lower). Agarose beads are conjugated with reverse primer targeting the human GAPDH gene, while the corresponding forward primer is labeled with TAMRA. (C) Flow cytometry analysis of beads from emulsion droplet bead PCR, starting with 1 *Escherichia coli* K12 cell/droplet (upper) and 0 *E. coli* K12 cell/droplet (lower). Reverse primer targeting the *gyr B* gene of *E. coli* is linked to agarose beads, and the forward primer is labeled with FAM.

Single cell genetic analysis was demonstrated using bacterial and mammalian cells at two different single cell dilutions. When mixed with microbeads, a uniform distribution of both intact cells and beads in the droplets is observed. Figure 6A (inset) presents an optical image of a droplet in the channel containing one human lymphocyte cell and one bead. The 10 min hot start step for polymerase activation at the beginning of PCR also serves to completely lyse the cells and release the genomic DNA into the droplet volume. In the first single cell experiment, a 419 bp region of the GAPDH (glyceraldehyde 3 phosphate dehydrogenase) gene in human lymphocyte cells was targeted and the cells were introduced at an average concentration of 0.1 cell per 2.5 nL droplet. For these cell and bead concentrations, 9.5% of the total processed beads should fluoresce due to the product as predicted by the Poisson distribution. Flow cytometry results (Figure 6B) show that 8.5% of the total bead population is strongly fluorescent. This good yield correspondence indicates that the products are the result of successful single cell amplifications. In the second single cell experiment, bacterial *E. coli* K12 cells were used and a 176 bp region of the *gyr B* gene was targeted. At an arbitrarily selected 1 cell/droplet concentration, Poisson statistics predict 63% of the processed beads should fluoresce. The flow cytometry results (Figure 6C) show 57% of the beads fluoresce, again consistent with successful single bacterial cell genetic amplification.

DISCUSSION

μDG, the Core Engine for SCGA. Using the μDG, we have demonstrated high-throughput processing of individual microbeads together with DNA and cell templates in uniform nanoliter PCR reactions. Linking the PCR progeny generated from a single DNA molecule or a single cell to primer functionalized microbeads is critical for efficient high-throughput downstream manipulation and analysis. Transitioning from the monolithic substrate used in earlier droplet generators[20,22] to a hybrid multilayer glass−PDMS assembly enables on-chip pumping with PDMS membrane valves, which are more effective in transferring beads (obviating bead settlement within the syringe), and greatly minimizes the reactive glass surface area contacted by the PCR reagent. In addition, the pulsatile nature of on-chip valve pumping provides precise control over droplet generation frequency due to the correspondence of the pulses with droplet formation. Hence, droplet size and volume fraction are exactly determined by varying controlled physical parameters such as the pump size, actuation pressure/vacuum, and intervals. This control is crucial for generating droplets in the optimum volume range for thermostability, for keeping the effective concentration of the single copy DNA template high within the droplet (~fM), and to ensure the correct quantity of starting reagents for efficient long-range DNA amplification. Previously presented large-scale single copy amplification via microfluidic digital PCR,[29] real-time single copy PCR in picoliter droplets,[16] as well as other platforms that produce droplets in the femtoliter to picoliter range cannot uniformly amplify sufficient amounts of long templates required by next generation sequencing platforms and/or do not allow facile downstream processing and manipulation of the products from the individual reactions. Thus with SCGA, we demonstrate the unique ability to efficiently amplify long individual DNA templates with high yields in a high-throughput fashion that facilitates downstream processing and analysis.

The composition of the emulsion oil is critical for biocompatibility and for ease of droplet formation. Although the emulsion oil used here has previously been used for single DNA template amplification via conventional agitation-based emulsion generation[10] and readily forms droplets in our μDG, it was found to swell PDMS on contact, thus rendering the device unusable. To address this problem, the oil in our microdevice is directly infused using syringe pumps into all-glass channels. Microfines have been found

(29) Ottesen, E. A.; Hong, J. W.; Quake, S. R.; Leadbetter, J. R. *Science* **2006**, *314*, 1464–1467.

to be important for enhancing reaction stability during PCR; however, no explanation was provided.[10] Our droplets were collected in a microfine solution as well, and this was found to be critical for successful PCR. Microfines assemble around the droplets during thermal cycling, and this is correlated with a lack of PCR inhibition. Further, droplets can also be formed using the microfine solution instead of the oil, and results from both techniques were comparable.

SCGA for Sequencing Template Preparation. New whole genome short-read sequencing technologies[10,11] use conventional agitation-based emulsion PCR techniques for high-throughput single molecule DNA amplification of clonal libraries. This emulsification process involves aggressively stirring[30,31] or agitating[10] the aqueous and oil phases together to spontaneously form aqueous droplets in oil whose sizes range from femtoliter to picoliter. However, these methods are fundamentally limited because neither approach can efficiently and uniformly amplify the long DNA amplicons, needed for complex genome assemblies, due to the extreme polydispersity of the droplets.[10] Typically, ~10 amol of short (~250 bp) amplicons are generated by these methods at best. In contrast, the monodisperse nanoliter emulsion droplets formed by the μDG hold ~10-fold excess primers and nucleotides (at standard PCR concentrations) required for the efficient generation of ~100 amol of >500 bp PCR amplicons. Because of the stochastic nature of nucleotide incorporation in pyrosequencing, the signal-to-noise varies as the square root of the total product on a bead. Thus, a 10-fold increase in the product per bead will result in a ~3-fold increase in signal-to-noise. This increase in S/N coupled with the production of longer templates should lead to a dramatic improvement in read lengths achieved by pyrosequencing.

The μDG is also a key engine for powering new whole genome long-read Sanger sequencing technologies based on single molecule amplification. The MINDS process we are developing consists of clonal library amplification on microbeads, followed by integrated Sanger extension from a single clonal microbead, reaction product purification, and sequencing separation using an integrated array of nanoliter volume processors and capillary electrophoresis (CE) channels. Toward this goal, we have successfully developed a bioprocessor that integrates the three most challenging Sanger sequencing processes: nanoliter-volume thermal cycling, product purification, and electrophoretic separation.[12] In addition, we recently achieved high-quality sequence data from only ~100 amol of PCR amplicon using an ultraefficient inline-injection microdevice.[13] With SCGA, we have now demonstrated the key front end of the MINDS process by producing over 100 amol of >500 bp product on a single bead starting from a single template copy. Furthermore, the generation of high-quality Sanger sequence data from a >600 bp product amplified on these beads shows that the amplicons produced here are viable Sanger sequencing templates. This achievement establishes the feasibility of SCGA for single molecule clonal library amplification required by the MINDS process.

Single Cell Genetic Analysis. The ability to manipulate and genetically analyze large numbers of single cells will enable novel studies of pathogenesis and a better understanding of the stochastic molecular mechanisms underlying cellular functions.[32] Agitation-based emulsification techniques[24] are not suitable for high-throughput single cell studies because the cells are disrupted before their successful compartmentalization. Intact cells have been optically trapped into emulsion droplets[21] but the process is time-consuming, requires an expensive optical setup, and is not high-throughput. In contrast, cells can be efficiently isolated and compartmentalized in emulsion droplets with our μDG. In a four-hour run, a single μDG can generate ~5000 "active" droplets containing a single microbead and a single intact cell. This μDG is also easily scaleable up to arrays of 96 generators as we have done for microfabricated CE, which should produce up to ~2 000 000 "active" droplets in 18 h. This high-throughput single cell processing capacity should, for instance, allow detection of extremely low concentrations (~1 in a 1 000 000) of somatic variants such as cancer cells present in circulation that result in increased mortality in solid-tumor patients.[33] Also, the clonal beads extracted from active droplets can be used for detailed genetic analysis of mutation, deletion, and translocation events at the single cell level. Rare disease-causing bacterial cells present in a background of nonpathogenic bacterial cells, such as one *E. coli* O157:H7 among 100 000s of *E. coli* K12 cells, or drug resistant *Staphylococcus aureus* in a normal bacterial background could be detected and analyzed within hours through digital processing of individual events.

A key attribute of the μDG for single cell analysis is its ability to incorporate functionalized beads into uniform nanoliter droplets. It is critical to compartmentalize single cells in uniform reactors with the same amount of reactants for a quantitative comparison of the products. The monodisperse droplets produced by the μDG should also enable large-scale quantitative comparison of mRNA expression at the single cell level, single-cell protein quantitation,[34] and single-cell enzymatic assaying.[21,35] All of these applications will digitally reveal low-level variations occurring within populations of seemingly identical cells. Such variations have been previously masked by population averaging of homogenized samples or by the inability to analyze large numbers of individual cells.

CONCLUSION

The past few years have seen an explosion in the understanding and use of microemulsions for high-throughput, ultralow volume studies of chemical and biological processes. Engineered emulsion based analysis platforms are going to be consequential in the development of large scale quantitative studies of genetic and other variations through massively parallel single molecule and single cell studies. The results presented here establish technologies that will enable the acquisition of this digital genetic information and thus elucidate the importance of stochastic variations in biological function.

ACKNOWLEDGMENT

P.K. and C.J.Y. contributed equally to this work. We acknowledge thoughtful discussions with Emory Chan and Nicholas

(30) Tawfik, D. S.; Griffiths, A. D. *Nat. Biotechnol.* **1998**, *16*, 652–656.
(31) Ghadessy, F. J.; Ong, J. L.; Holliger, P. *Proc. Natl. Acad. Sci. U.S.A.* **2001**, *98*, 4552–4557.
(32) Sims, C. E.; Allbritton, N. L. *Lab Chip* **2007**, *7*, 423–440.
(33) Krivacic, R. T.; Ladanyi, A.; Curry, D. N.; Hsieh, H. B.; Kuhn, P.; Bergsrud, D. E.; Kepros, J. F.; Barbera, T.; Ho, M. Y.; Chen, L. B.; Lerner, R. A.; Bruce, R. H. *Proc. Natl. Acad. Sci. U.S.A.* **2004**, *101*, 10501–10504.
(34) Huang, B.; Wu, H. K.; Bhaya, D.; Grossman, A.; Granier, S.; Kobilka, B. K.; Zare, R. N. *Science* **2007**, *315*, 81–84.
(35) Cai, L.; Friedman, N.; Xie, X. S. *Nature* **2006**, *440*, 358–362.

Toriello. Microfabrication was carried out at the University of California, Berkeley, Microfabrication Laboratory. This work was supported in part by National Institute of Health (NIH) Grant HG003583 via Microchip Biotechnologies, Inc. and by the trans-NIH Genes, Environment and Health Initiative, Biological Response Indicators of Environmental Stress Center Grant U54 ES016115-01. R.A.M. has a financial interest in Microchip Biotechnologies, which is commercially developing aspects of the technologies presented here.

SUPPORTING INFORMATION AVAILABLE

Additional information as noted in text. This material is available free of charge via the Internet at http://pubs.acs.org.

Received for review February 15, 2008. Accepted March 21, 2008.

AC800327D